CGI-58 facilitates the mobilization of cytoplasmic triglyceride for lipoprotein secretion in hepatoma cells[S]

J. Mark Brown,* Soonkyu Chung,* Akash Das,† Gregory S. Shelness,* Lawrence L. Rudel,*,† and Liqing Yu[1,*]

Department of Pathology, Section on Lipid Sciences,* and Department of Biochemistry,† Wake Forest University School of Medicine, Winston-Salem, NC 27157-1040

Abstract Comparative Gene Identification-58 (CGI-58) is a member of the α/β-hydrolase family of proteins. Mutations in the human CGI-58 gene are associated with Chanarin-Dorfman syndrome, a rare autosomal recessive genetic disease in which excessive triglyceride (TG) accumulation occurs in multiple tissues. In this study, we investigated the role of CGI-58 in cellular lipid metabolism in several cell models and discovered a role for CGI-58 in promoting the packaging of cytoplasmic TG into secreted lipoprotein particles in hepatoma cells. Using both gain-of-function and loss-of-function approaches, we demonstrate that CGI-58 facilitates the depletion of cellular TG stores without altering cellular cholesterol or phospholipid accumulation. This depletion of cellular TG is attributable solely to augmented hydrolysis, whereas TG synthesis was not affected by CGI-58. Furthermore, CGI-58-mediated TG hydrolysis can be completely inhibited by the known lipase inhibitors diethylumbelliferyl phosphate and diethyl-*p*-nitrophenyl phosphate, but not by *p*-chloro-mercuribenzoate. Intriguingly, CGI-58-driven TG hydrolysis was coupled to increases in both fatty acid oxidation and secretion of TG. Collectively, this study reveals a role for CGI-58 in coupling lipolytic degradation of cytoplasmic TG to oxidation and packaging into TG-rich lipoproteins for secretion in hepatoma cells.—Brown, J. M., S. Chung, A. Das, G. S. Shelness, L. L. Rudel, and L. Yu. **CGI-58 facilitates the mobilization of cytoplasmic triglyceride for lipoprotein secretion in hepatoma cells. *J. Lipid Res.* 2007.** 48: **2295–2305.**

Supplementary key words Comparative Gene Identification-58 • triglyceride hydrolysis • lipolysis

The ability to store excess energy in the form of triglyceride (TG) is a critical defense mechanism to help organisms survive extended periods of fuel deprivation. Therefore, elegant systems have evolved to facilitate the storage of excess energy into adipose tissue in the form of TG-rich lipid droplets (LDs) or "adiposomes" (1). Although adipocytes have the unique ability to store large amounts of cytoplasmic TG, almost all tissues can synthesize and store TG in smaller cytoplasmic LDs under normal and pathologic conditions (2–4). The metabolic fate of TG in cytoplasmic LDs differs among cell types (3, 5–8). Hepatocytes in the liver and enterocytes in the intestine are lipoprotein-producing cells, having the unique ability to efficiently package lipid cargo into apolipoprotein B (apoB)-containing lipoproteins that ultimately deliver these lipids to all peripheral tissues. This assembly of apoB-containing lipoproteins is widely accepted as a two-step process (7, 8). The first step involves the cotranslational transfer of a small amount of phospholipids (PLs) and TGs to apoB by the actions of microsomal triglyceride transfer protein (MTP). This step results in a small dense precursor particle (~25 nm) residing within the endoplasmic reticulum (ER) lumen. The more elusive second step involves the bulk addition of TG to these precursor particles to form large (30–80 nm) secretion-competent VLDLs. This second step expansion occurs through an obscure process involving *1*) the lipolysis of cytoplasmic LD-associated TG, *2*) the movement of liberated acylglycerols toward the ER, and *3*) the reesterification of acylglycerols to form a large lumenal TG-rich droplet that fuses with the smaller apoB-containing first-step particle (9–12). Molecular mechanisms to determine whether cytoplasmic LD-associated TG is directed to lipoproteins for secretion or into lipid storage LDs are currently unknown.

More than 30 years ago, two independent investigators [Chanarin et al. (13) and Dorfman et al. (14)] discovered

Abbreviations: ADRP, adipose differentiation-related protein; apoB, apolipoprotein B; ATGL, adipose triglyceride lipase; CDS, Chanarin-Dorfman syndrome; CE, cholesteryl ester; CGI-58, Comparative Gene Identification-58; DEUP, diethylumbelliferyl phosphate; E-600, diethyl-*p*-nitrophenyl phosphate; EGFP, enhanced green fluorescent protein; ER, endoplasmic reticulum; IDL, intermediate density lipoprotein; iPLA2ζ, calcium-independent phospholipase A2ζ; LD, lipid droplet; MTP, microsomal triglyceride transfer protein; PCMB, *p*-chloro-mercuribenzoate; PL, phospholipid; siRNA, short interfering RNA; TG, triglyceride.

[1] To whom correspondence should be addressed.
e-mail: lyu@wfubmc.edu

[S] The online version of this article (available at http://www.jlr.org) contains supplementary data in the form of 2 figures.

Manuscript received 14 June 2007 and in revised form 23 July 2007.
Published, JLR Papers in Press, July 30, 2007.
DOI 10.1194/jlr.M700279-JLR200

an autosomal recessive disease in humans that manifested as massive TG deposition in multiple tissues. This condition was originally described as neutral lipid storage disease and was more recently named Chanarin-Dorfman syndrome (CDS). Extensive clinical examination of CDS patients revealed several lipid-associated pathologies, including ichthyosis, hepatic steatosis, cardiomyopathy, ataxia, and mental retardation (15–18). Several elegant studies done using fibroblasts derived from CDS patients demonstrated that the excess TG accumulation in these cells did not result from augmented fatty acid uptake or TG synthesis rates (19, 20). Instead, fibroblasts from CDS patients seem to lack the ability to hydrolyze stored TG, even though cellular lipase and carboxylesterase activities are normal (20–22). As a result of this paradoxical finding, it has been speculated that TG lipases in these cells may be missing some critical cofactor, be mislocalized, or be unable to gain access to the LD surface (23, 24). This paradox may be partially explained by the fact that CDS fibroblasts exhibit abnormal recycling of TG-derived monoacylglycerols or diacylglycerols into major PL species (25, 26).

Indeed, in 2001, the genetic mutation and the speculated "missing cofactor" (23, 24) was identified as Comparative Gene Identification-58 (CGI-58) (27), also known as α/β-hydrolase domain-containing 5. Several studies have since confirmed that multiple loss-of-function mutations in CGI-58 are causative of CDS (28–31). However, CGI-58's role in cellular TG metabolism has yet to be completely elucidated. Initial studies have demonstrated that CGI-58 localizes to intracellular LDs through a direct interaction with perilipin (1, 32, 33). However, in these studies, a significant portion of CGI-58 was found to be localized to a poorly defined non-LD compartment (32, 33). Further studies have demonstrated that CGI-58 facilitates lipolysis by acting as a coactivator for adipose triglyceride lipase (ATGL) in adipocytes (34, 35). However, these studies left several questions unresolved regarding the role of CGI-58 in TG hydrolysis in tissues that express undetectable levels of ATGL (e.g., liver) and whether CGI-58 plays a quantitatively important role in adipose tissue lipolysis, because CDS patients display normal adiposity (27–31). Importantly, CGI-58 is abundantly expressed in mouse liver (33, 34), yet its role in hepatocyte TG metabolism remains obscure. In this study, we examined the role of CGI-58 in the mobilization of cytoplasmic TG for lipoprotein secretion. The results demonstrate that CGI-58 is an important component of the lipolysis/reesterification cycle that drives the packaging of TG into nascent lipoprotein particles in hepatoma cells.

MATERIALS AND METHODS

Materials

We obtained (1-^{14}C]oleic acid (NET-317), [9,10-^{3}H(N)]oleic acid (NET-289), and Western Lightning Plus Chemiluminescence Substrate from Perkin-Elmer Life Sciences (Waltham, MA); the bicinchoninic acid protein assay kit from Pierce (Rockford, IL); Trizol, NuPAGE precast gels, ER-Tracker Blue-White DPX (E-12353), MitoTracker Deep Red 633 (M-22426), Alexa Fluor 594-conjugated lectin GS-II (L-21416), and ProLong Antifade Kit (P-7481) from Invitrogen (Carlsbad, CA); Immobilon P polyvinylidene difluoride membranes from Millipore (Billerica, MA); and rubber stoppers and an inverted center well hanging bucket for oxidation assays from Kontes Glass Co. (Vineland, NJ). All oligonucleotide primers were from Integrated DNA Technologies (Coralville, IA); control nontargeting short interfering RNA (siRNA), siGLO, CGI-58 siRNA ON-TARGETplus pool (Rat LOC316122), and transfection reagent (DharmaFECT-1) were from Dharmacon (Lafayette, CO). Takara LA *Taq* polymerase was from Takara Bio (Shiga, Japan). All restriction endonucleases and pGEM-T Easy were from Promega (Madison, WI); pEGFP-N1 vector was from Clontech (Mountain View, CA). Nucleofector and all transfection reagents (Kit V = VCA-1003; Kit T = VCA-1002) were obtained from Amaxa (Gaithersburg, MD); TG (Triglycerides/GB) and total cholesterol (Total Cholesterol Reagent) enzymatic kits from Roche (Switzerland); and free cholesterol (Free Cholesterol C) and PLs (Phospholipid C) enzymatic kits from Wako Chemical (Richmond, VA). The mouse monoclonal antibody for Akt-1 (2967) was from Cell Signaling Technologies (Beverly, MA), monoclonal anti-adipose differentiation-related protein (ADRP) antibody was from Research Diagnostics (Concord, MA), and Cy3-conjugated goat anti-mouse secondary antibody was from Jackson Immunoresearch (West Grove, PA). Omniscript reverse transcriptase was obtained from Qiagen (Valencia, CA), and Ready-To-Go T4 DNA ligase was from GE Healthcare (Piscataway, NJ). All other reagents were purchased from Sigma, unless stated otherwise.

Cloning of human CGI-58 cDNA and construction of enhanced green fluorescent protein-tagged expression vector

A human CGI-58 cDNA was amplified out of a random hexamer-primed cDNA pool generated by reverse-transcribing 1 μg of total RNA isolated from primary cultures of human adipocytes (kindly provided by Dr. Michael McIntosh, University of North Carolina at Greensboro). Cloning of the full-length CGI-58 or a version missing the stop codon (for fusion protein generation) from this pool was accomplished by PCR using Takara LA *Taq* polymerase and primer pairs 5′-CGTAAAGCTTCGGCTATGGCGGCGGAGGAG-3′ and 5′-GTAGCGGCCGCAGTATAGTCAAGAAGGCTG-3′ for full-length cDNA generation or 5′-CGTACCGCGGGTCCACAGTGTCGCAGATCT-3′ to delete the stop codon for fusion protein generation. *Hind*III (5′) and *Sac*II (3′) or *Not*I (3′) restriction sites were added for directional cloning purposes. Resulting PCR products were cloned directly into the pGEM-T Easy vector (Promega) and sequenced using T7, SP6, and gene-specific primers. The resulting plasmid pGEM-*Hind*III-hCGI-58-*Sac*II lacking the stop codon was digested with *Hind*III and *Sac*II endonucleases to release the hCGI-58 insert, which was subcloned into *Hind*III-*Sac*II-cut pEGFP-N1 (Clontech) using Ready-To-Go T4 DNA Ligase. The resultant recombinant plasmid, designated pEGFP-hCGI-58, was verified by restriction mapping and sequencing.

Cell culture

CHO-K1 cell lines were maintained at 37°C in 5% CO_2 in medium A [Ham's F-12 medium supplemented with 1% Eagle's vitamins, penicillin (100 U/ml), streptomycin (100 μg/ml), and 10% heat-inactivated FBS], and cells were typically grown to 70–90% confluence for all experiments. All other cells lines, HepG2, McA-RH7777, and COS-1, were maintained at 37°C in 5% CO_2 in medium B [DMEM with 4.5 g/l glucose, 1% Eagle's

vitamins, penicillin (100 U/ml), streptomycin (100 μg/ml), and 10% heat-inactivated FBS]. COS-1 and HepG2 cells were typically grown to 70–90% confluence, whereas McA-RH7777 cells were maintained at ~40–70% confluence to ensure the health of cells.

Transient and stable overexpression of enhanced green fluorescent protein or hCGI-58-enhanced green fluorescent protein in multiple cell lines

CHO-K1, COS-1, HepG2, and McA-RH7777 cells were trypsinized, and 2×10^6 cells were nucleofected with 5 μg of pEGFP-N1 or pEGFP-hCGI-58 plasmids according to Amaxa's instructions with the following minor modifications. For CHO-K1 transfections, cell pellets were resuspended in 100 μl of solution T and nucleofected using program O-017. Stable cell populations were selected in culture medium containing 800 μg/ml G418, and several monoclonal lines expressing enhanced green fluorescent protein (EGFP) or CGI-58-EGFP were isolated by ring cloning. For COS-1, HepG2, and McA-RH7777 transient transfections, cell pellets were resuspended in 100 μl of solution V and nucleofected using program T-028.

siRNA-mediated silencing of endogenous CGI-58 in McA-RH7777 hepatoma cells

McA-RH7777 cells were seeded at a density of 5×10^5 cells per plate on 35 mm dishes and maintained in medium B for 24–48 h. Thereafter, cells were transfected with 100 nM of a red fluorescent (Cy3)-tagged nontargeting siRNA (siGLO), a nontargeting siRNA (control siRNA), or a pool of four individual siRNAs targeting rat CGI-58, according to Dharmacon's instructions. At 24 h after transfection, efficiency was determined using siGLO, and at 48 h after transfection, all other analyses were conducted.

Measurement of cellular lipid mass

COS-1, HepG2, or McA-RH7777 cells were transiently transfected with plasmids driving the expression of either EGFP or hCGI-58-EGFP as described above and seeded on 100 mm dishes. At 48 h after transfection, cells were maintained in either the absence or presence of 0.8 mM oleic acid (complexed to fatty acid-free BSA at a 4:1 molar ratio) in medium B for an additional 24 h to drive cellular TG accumulation. Thereafter, total lipids were extracted using the method of Bligh and Dyer (36), and lipid mass was determined enzymatically as described previously (37).

Radiolabeling cellular and secreted lipids

CHO-K1, COS-1, HepG2, or McA-RH7777 cells were transfected as described above, seeded on 35 mm plates, and grown until 60–90% confluence was reached (usually 24–48 h after transfection). In some cases, the cells were pretreated for 1 h with several known (24, 38–40) inhibitors of TG or cholesteryl ester (CE) hydrolysis, including diethylumbelliferyl phosphate (DEUP), diethyl-*p*-nitrophenyl phosphate (E-600), and *p*-chloro-mercuribenzoate (PCMB). Hydrolase inhibitor stocks were made up as follows: DEUP was solubilized in DMSO (50 mg/ml); E-600 was dissolved in water (2.5 mg/ml); and PCMB (25 mM) was dissolved in 0.1 M NaOH. Cells were then pulse-labeled in normal growth medium (medium A for CHO-K1, medium B for all others) with or without hydrolase inhibitors by adding 5 μCi/ml [^{3}H]oleic acid and, in some cases, 0.8 mM cold oleic acid to stimulate TG secretion. In the pulse-chase experiment described in Fig. 6C below, siRNA-transfected McA-RH7777 cells were pulse-labeled in medium B containing 5 μCi/ml [^{3}H]oleic acid for 24 h, washed gently twice with balanced salt solution, and chased in medium B containing 1 μCi/ml [^{14}C]oleic acid plus 0.8 mM cold oleic acid to stimulate VLDL-TG secretion for another 4 h. After the radiolabeling period, 1 ml of conditioned medium was collected and adjusted to a density of either 1.225 or 1.063 g/ml. The samples were loaded into a Quick-seal tube (Beckman) and overlaid to the top with the appropriate density solution. Samples were centrifuged at 100,000 rpm in a Beckman TL-100 ultracentrifuge using a TLA-120.2 rotor for 18 h at 15°C. The top 300 μl [$d < 1.225$ g/ml = total lipoprotein fraction; $d < 1.063$ g/ml = VLDL, intermediate density lipoprotein (IDL), and LDL] or the bottom 1.7 ml ($d > 1.063$ g/ml = small dense particles) fractions were recovered by tube slicing. Total lipid extracts were made from media fractions and cells using the method of Bligh and Dyer (36). Thereafter, carrier standards were added to samples and lipid classes were separated by TLC using Silica Gel 60 plates and a solvent system containing hexane-diethyl ether-acetic acid (70:30:1). Lipids were visualized by exposure to iodine vapor, and bands corresponding to CE, TG, and PL were scraped and counted. Protein concentration of parallel cultures was determined using the bicinchoninic acid assay.

Measurement of fatty acid oxidation

HepG2 or McA-RH7777 cells were transfected with expression vectors or siRNA, respectively, to modulate CGI-58 expression as described above. Fatty acid oxidation was measured as described previously (41).

Immunoblot analysis

Postnuclear supernatants were generated and used to perform Western blot analysis as described previously (42). The following primary antibodies were used: *1*) mouse monoclonal antibody for Akt-1; *2*) rabbit anti-rat-CGI-58 sera (32) (kindly provided by Dr. Takashi Osumi, University of Hyogo, Japan); and *3*) rabbit anti-mouse-CGI-58 sera (33) (kindly provided by Dr. Dawn Brasaemle, Rutgers University, New Brunswick, NJ).

Quantitative real-time PCR

Total RNAs were extracted from C57BL/6J male mouse or African green monkey tissues using either the RNA Stat-60 kit (Tel-Test, Inc., Friendswood, TX) or Trizol, respectively. Real-time PCR was performed on pooled cDNA samples from three animals for each tissue, and quantitative real-time PCR was performed as described previously (43, 44) using primers 5′-TGGTAAAATGCACCCTGACA-3′ and 5′-CAGTCCACAGTGTCGCAGAT-3′ for monkey CGI-58, 5′-TGACAGTGATGCGGAAGAAG-3′ and 5′-AGATCTGGTCGCTCAGGAAA-3′ for mouse and rat CGI-58, and 5′-TGACTCAACACGGGAAACCTCAC-3′ and 5′-TCGCTCCACCAACTAAGAACGG-3′ for 18S rRNA.

Immunofluorescence microscopy

For ADRP and Golgi staining, cells were fixed with 3.7% paraformaldehyde in PBS for 20 min, then the coverslips were quenched and permeablized with 0.1% saponin, 10 mM glycine, and 1.25 mg/ml goat IgG in PBS for 1 h. Immunodetection of ADRP was carried out by incubating cells with a 1:50 dilution of mouse anti-ADRP for 12 h at 4°C, followed by 4 μg/ml Cy3-conjugated goat anti-mouse secondary antibody incubation for 1 h. For Golgi apparatus staining, permeabilized cells were incubated with a 1:1,500 dilution of Alexa Fluor 594-conjugated lectin GS-II for 1 h. Coverslips were washed three times with PBS and incubated with 1 μg/ml 4′6-diamidino-2-phenylindole (DAPI) for 5 min for nuclei staining. After an additional three washes, coverslips were mounted on glass slides using the ProLong Antifade Kit. To visualize ER and mitochondria, live

cells were incubated with 1 μM ER-Tracker Blue-White DPX and 500 nM MitoTracker Deep Red 633 for 30 min each according to the manufacturer's protocol. Both fixed and live images were captured with a SPOT digital camera mounted on an Olympus BX60 fluorescence microscope. Live images of mitochondria were acquired using a CSU-10 confocal microscope.

Statistical analysis

Unless indicated otherwise, data are expressed as means ± SEM. All data were analyzed using one-way ANOVA followed by Student's *t*-tests for each pair for multiple comparisons. Differences were considered significant at $P < 0.05$. All analyses were performed using JMP version 5.0.12 software (SAS Institute, Cary, NC).

RESULTS

CGI-58 mRNA is expressed ubiquitously, yet relative abundance in tissues varies among species

To determine the relative expression level of CGI-58 in the liver, the tissue distribution of CGI-58 was examined in mice and monkeys. Using quantitative real-time PCR, we confirmed previous findings (33, 34) that CGI-58 is expressed in almost all mouse tissues examined (**Fig. 1**), with the most abundant expression by far seen in testes. The rank order of CGI-58 mRNA levels in mouse tissues is as follows: testes, adipose tissue, heart, kidney, adrenal gland, muscle, skin, stomach, liver, ileum, colon, cerebrum, jejunum, whole brain, spleen, duodenum, and lung. In African green monkeys, the most abundant expression of CGI-58 was evident in the small intestine and adrenal gland, yet CGI-58 was detected in all tissues examined. The rank order of CGI-58 mRNA levels in monkey tissues is as follows: small intestine, adrenal gland, adipose tissue, skin, skeletal muscle, brain, diaphragm, testes, kidney, lung, liver, spleen, lymph node, and aorta. PCR amplicons from monkey liver cDNA samples were confirmed to be CGI-58 by sequencing.

CGI-58-EGFP fusion proteins localize to LDs, the ER, and the Golgi apparatus

To study the subcellular localization of CGI-58, we expressed CGI-58 as a fusion protein with EGFP appended to its C terminus in multiple cell lines. The data shown in

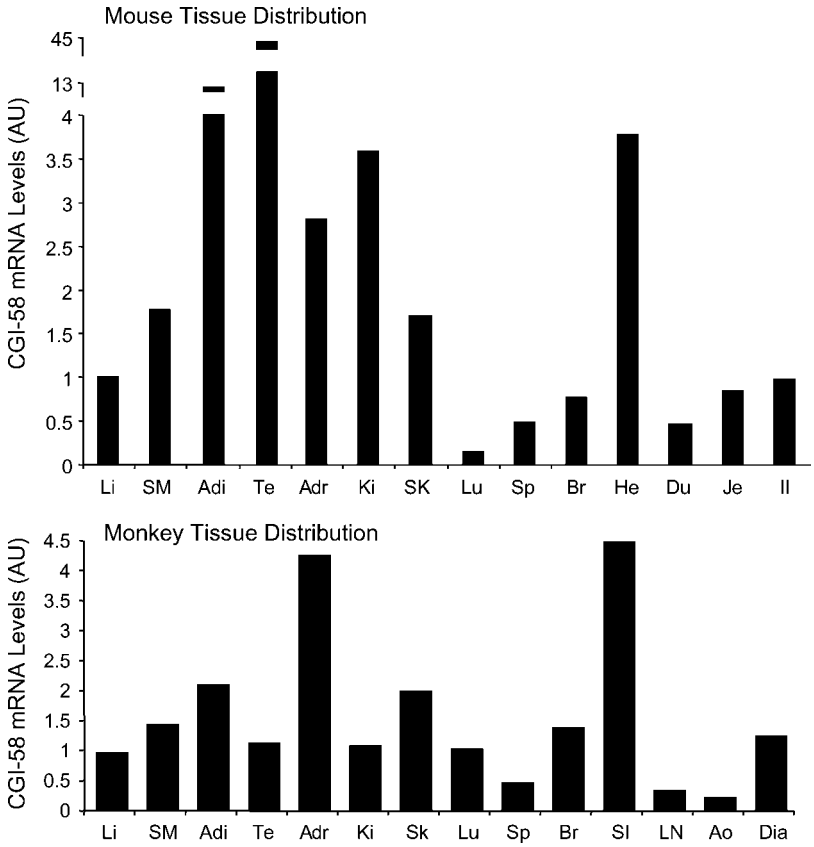

Fig. 1. Expression of Comparative Gene Identification-58 (CGI-58) mRNA in mouse and monkey tissues. Quantitative real-time PCR was conducted to detect the relative expression levels of CGI-58 mRNA transcripts in mouse (top) and African green monkey (bottom) tissues. CGI-58 abundance was normalized to 18S rRNA levels and is expressed as fold change compared with the liver expression level, which was arbitrarily set to 1. Lane designations are as follows: Li, liver; SM, skeletal muscle; Adi, adipose tissue; Te, testes; Adr, adrenal gland; Ki, kidney; SK/Sk, skin; Lu, lung; Sp, spleen; Br, brain; He, heart; Du, duodenum; Je, jejunum; Il, ileum; SI, small intestine; LN, lymph node; Ao, aorta; Dia, diaphragm. Data are representative of triplicate measurements in pools from three individual animals. AU, arbitrary units.

Fig. 2 represent images captured using CHO-K1 cells stably expressing EGFP or CGI-58-EGFP, but the subcellular localization was similar in all cell lines tested (COS-1, HepG2, McA-RH7777, Huh7). In CHO-K1 cells, stable expression of EGFP resulted in uniform diffuse localization (Fig. 2A, panels 7, 10). By contrast, CGI-58-EGFP fusion proteins localized to distinct perinuclear punctate structures and what seemed to be vesicular structures throughout the cytoplasm (Fig. 2A, panel 1, and Fig. 2B, panels 1, 7, 13). Importantly, a small proportion of CGI-58-EGFP colocalized with the LD marker protein ADRP, but the majority of CGI-58 remained in a non-ADRP-containing compartment (Fig. 2A, panel 3). Interestingly, when CGI-58-EGFP cells were grown in normal medium containing 10% FBS, the immunostaining of ADRP was much less intense compared with that in cells overexpressing EGFP (Fig. 2A, compare panels 2 and 8). This is likely attributable to the fact that CGI-58-EGFP overexpression results in significant reductions in cellular TG mass (**Fig. 3**), and ADRP is known to be posttranslationally stabilized by cytoplasmic TG (45).

When cells were stimulated with 0.8 mM oleic acid to drive TG accumulation, CGI-58-EGFP fusion proteins seemed to be more concentrated on ADRP-positive LD structures, yet a significant portion remained in a non-LD-associated perinuclear site (Fig. 2A, panel 6). This movement was not seen with EGFP, which always exhibited diffuse localization (Fig. 2A, panel 12). To further define the non-LD compartment that CGI-58-EGFP proteins were localized to, we used markers for the ER (ER-Tracker Blue-White DPX), the Golgi apparatus (Alexa Fluor 594-conjugated lectin GS-II), or mitochondria (MitoTracker Deep Red 633). Interestingly, CGI-58-EGFP fusion proteins colocalized well with both the ER (Fig. 2B, panel 3) and the Golgi (Fig. 2B, panel 9) but shared very little colocalization with mitochondria (Fig. 2B, panels 15, 18). Both ER and Golgi localization of CGI-58-EGFP seemed to remain constant under oleate-stimulated conditions

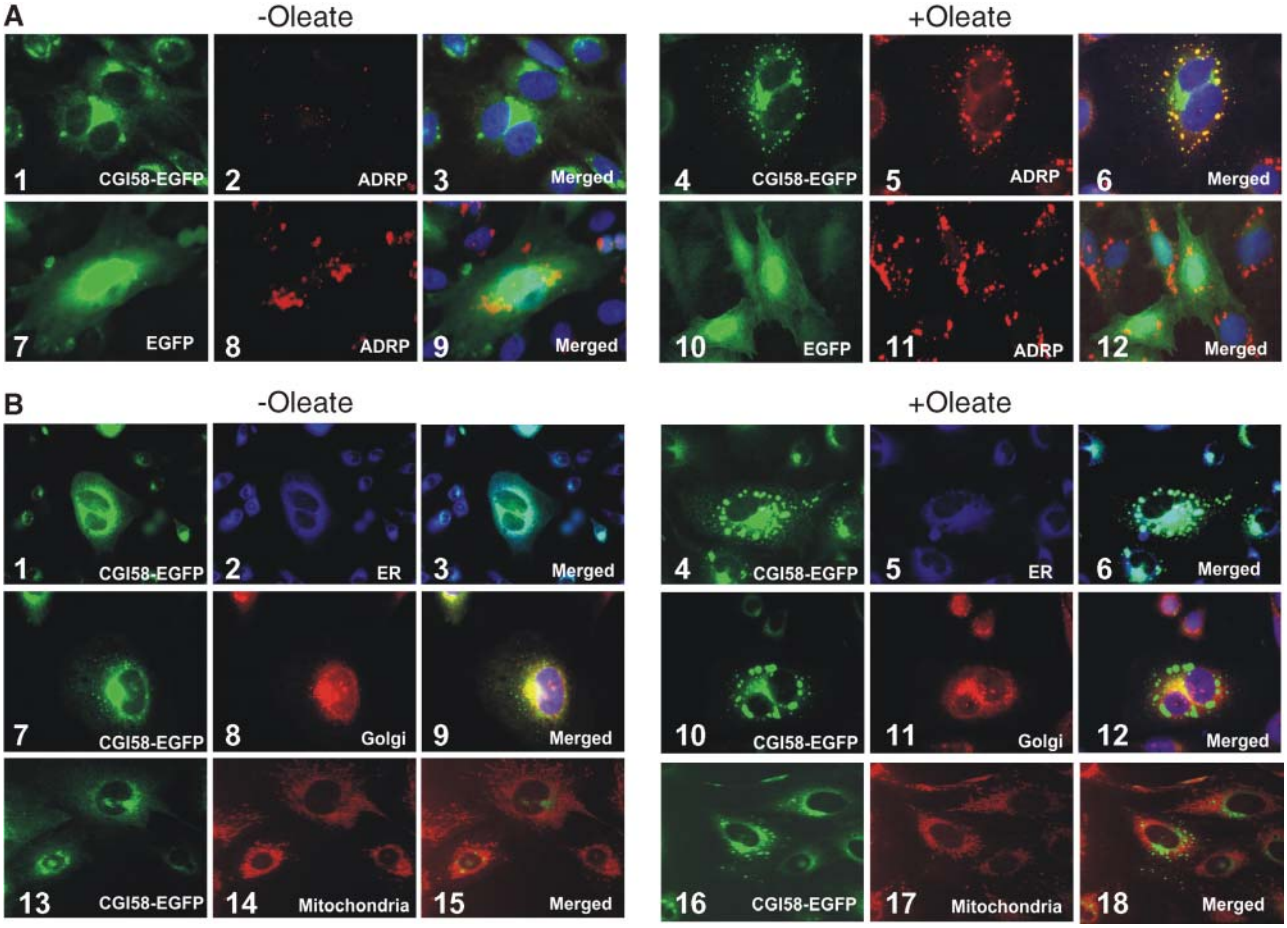

Fig. 2. CGI-58-enhanced green fluorescent protein (EGFP) proteins localize to lipid droplets (LD), Golgi apparatus, and endoplasmic reticulum (ER) compartments in stable CHO-K1 cells. Nonconfluent stable cell lines overexpressing EGFP or CGI-58-EGFP fusion proteins were kept in medium A without oleate (−Oleate) or with 0.8 mM oleic acid (+Oleate) to promote triglyceride (TG) accumulation in cells for 24 h, then either fixed or imaged in live cells as described in Materials and Methods. All green images represent CGI-58-EGFP fusion proteins. In A, the red signals represent adipose differentiation-related protein (ADRP) stained sequentially by the ADRP primary antibody and the Cy3 red-conjugated secondary antibody. The blue signals represent nuclei stained by 4′,6-diamidino-2-phenylindole. In B, red signals represent either Golgi stained by Alexa Fluor 594 (red)-conjugated lectin GS-II or mitochondria stained by MitoTracker Deep Red 633. The blue signals represent ER stained by ER-Tracker Blue-White DPX.

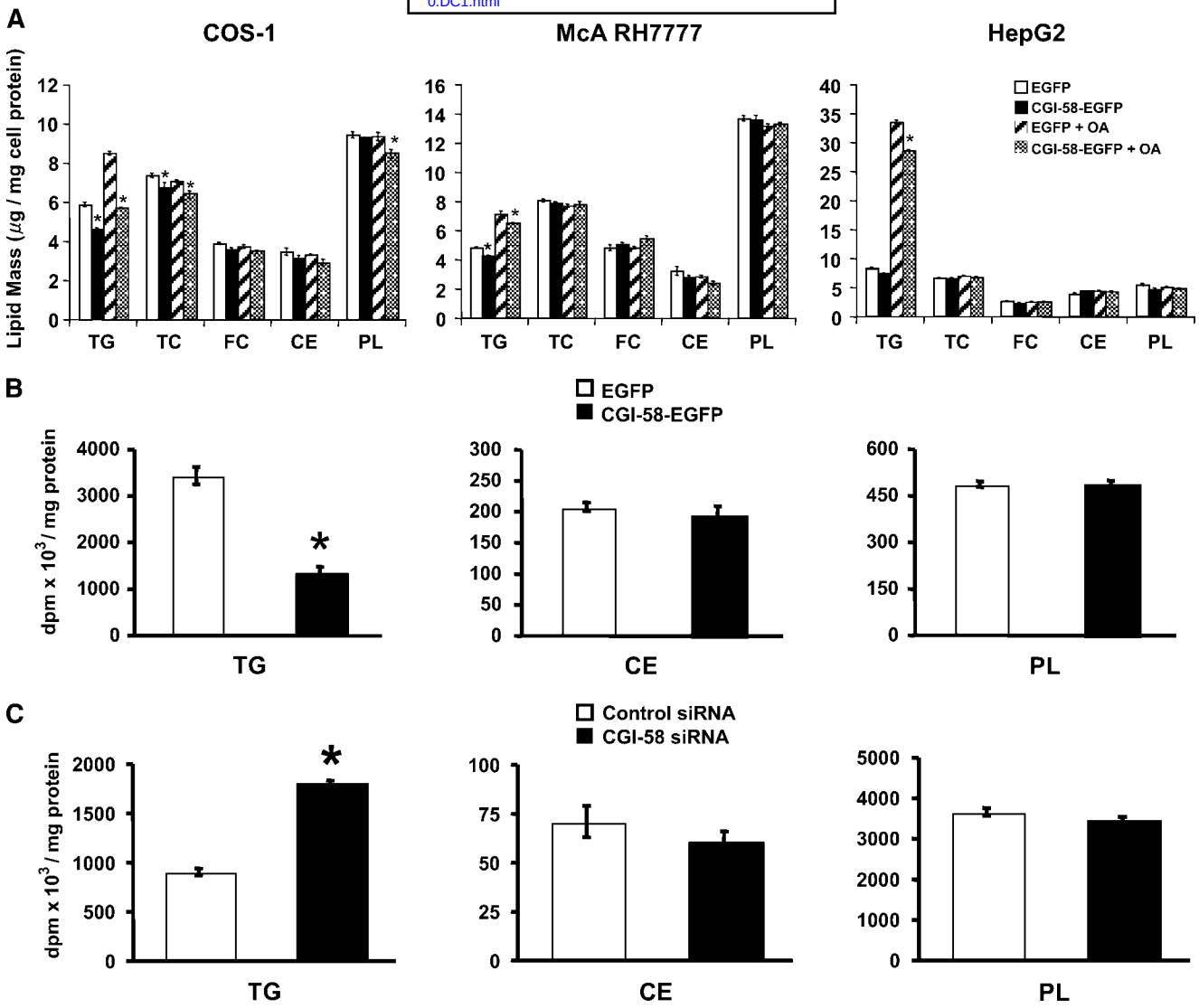

Fig. 3. CGI-58 promotes the specific depletion of cellular TG in multiple cell models. A: COS-1, McA-RH7777, and HepG2 cells were transiently transfected with plasmids encoding EGFP or CGI-58-EGFP fusion protein, and at 24 h after transfection cells were grown in the absence or presence of 0.8 mM oleic acid (+OA) for an additional 24 h to drive cellular TG accumulation. Thereafter, cellular TG, total cholesterol (TC), free cholesterol (FC), cholesteryl ester (CE), and phospholipid (PL) mass were determined. B: CHO-K1 cell lines stably overexpressing either EGFP or CGI-58-EGFP were pulse-labeled with 5 μCi of [^{3}H]oleic acid for 4 h in the presence of 0.8 mM cold oleic acid in medium A to drive TG accumulation. Thereafter, the incorporation of [^{3}H]oleic acid into TG, CE, and PL was determined. C: McA-RH7777 cells were transfected with 100 nM of either a nontargeting short interfering RNA (siRNA; Control siRNA) or a pool of siRNAs targeting the endogenous CGI-58 (CGI-58 siRNA). At 48 h after transfection, the cells were pulse-labeled with 5 μCi of [^{3}H]oleic acid for an additional 24 h in medium B. Thereafter, the incorporation of [^{3}H]oleic acid into TG, CE, and PL was determined. Data represent means ± SEM (n = 3 in A, C, n = 4 in B) from a representative experiment, which was repeated twice (A) or three times (B, C) with similar results. * $P < 0.05$ (CGI-58-EGFP vs. EGFP cells or CGI-58 siRNA vs. Control siRNA).

(Fig. 2B, panels 6, 12), whereas there was clear enrichment of CGI-58-EGFP in ADRP-positive LDs when oleate was given (Fig. 2A, panel 6).

CGI-58 promotes the specific depletion of cellular TG without affecting cholesterol or PL homeostasis

To define the role of CGI-58 in TG turnover, initial experiments were conducted using transient transfection to overexpress EGFP or CGI-58-EGFP in COS-1, McA-RH7777, or HepG2 cells. At 48 h after transfection, there was abundant overexpression of CGI-58-EGFP fusion protein in COS-1 cells, and the levels seen in McA-RH7777 and HepG2 cells were similar to the endogenous levels of CGI-58 in those cells (see supplementary Fig. I). CHO-K1 stable cell lines were also generated that overexpressed CGI-58-EGFP (see supplementary Fig. I). Interestingly, by overexpressing CGI-58-EGFP, the abundance of endogenous CGI-58 protein was increased (see supplementary Fig. I). This may be a result of posttranslational stabilization of the endogenous protein by interaction with the fusion protein. Importantly, as a result of CGI-58 overexpression (both fusion and endogenous), cel-

lular TG mass was reduced significantly in both COS-1 and McA-RH7777 cells (Fig. 3A). Furthermore, when cells were loaded with 0.8 mM oleic acid to drive TG accumulation, COS-1 cells overexpressing CGI-58-EGFP were protected against oleate-stimulated TG accumulation compared with cells expressing EGFP (Fig. 3A). In agreement, in McA-RH7777 and HepG2 cells expressing CGI-58-EGFP, there was significantly less oleate-stimulated TG mass compared with that in cells expressing EGFP (Fig. 3A). There was also a slight reduction in total cholesterol induced by CGI-58-EGFP overexpression in COS-1 cells, but this was not evident in other models tested.

The modest reductions in cellular TG mass seen in McA-RH7777 and HepG2 cell lines are likely explained by the transfection efficiencies in those cells: COS-1 (~70–80%), McA-RH7777 (~40%), and HepG2 (~50%). This conclusion is supported by the fact that in a monoclonal CHO-K1 cell line abundantly overexpressing CGI-58-EGFP in 100% of the cell population (see supplementary Fig. I), the accumulation of radiolabeled TG after a 4 h pulse-labeling with [^{3}H]oleic acid was reduced by 61% compared with EGFP control cells (Fig. 3B). Importantly, in this same experiment, radiolabeled CE and PL accumulation were not affected by CGI-58-EGFP (Fig. 3B). In further support of CGI-58's role in cellular TG metabolism, we were able to reduce endogenous CGI-58 mRNA and protein expression by 60–70% using siRNA (see supplementary Fig. II), and this resulted in a 2-fold increase in cellular TG accumulation without affecting CE or PL accumulation (Fig. 3C). Collectively, these data support the notion that CGI-58 is a critical player in cellular TG homeostasis and has very minor effects on either mass or [^{3}H]oleic acid incorporation into cellular CE or PL.

CGI-58-driven TG hydrolysis is mediated by a DEUP- and E-600-sensitive, but PCMB-insensitive, TG lipase

Because overexpression of CGI-58-EGFP resulted in decreased TG accumulation in all cell lines tested (Fig. 3), we investigated whether the CGI-58-mediated reduction in cellular TG content was attributable to an increased rate of turnover of TG or decreased synthesis. To examine TG synthesis without the complications of simultaneous turnover, we used known inhibitors (DEUP, E-600, and PCMB) of TG and CE hydrolases (24, 38–40). Stable CHO-K1 cell lines overexpressing EGFP or CGI-58-EGFP that had been pretreated with DEUP or E-600 showed an increased accumulation of [^{3}H]TG after 4 h of pulse-labeling (**Fig. 4**) compared with vehicle-treated cells. However, cells pretreated with PCMB did not have an increased accumulation of [^{3}H]TG compared with vehicle-treated cells. Importantly, vehicle-treated cells overexpressing CGI-58-EGFP accumulated 44% less [^{3}H]TG compared with vehicle-treated EGFP control cells (Fig. 4). Similarly, PCMB-treated cells overexpressing CGI-58-EGFP also accumulated 51% less [^{3}H]TG compared with PCMB-treated EGFP control cells (Fig. 4). In contrast to this, DEUP- and E-600-pretreated cells completely lacked CGI-58-driven TG hydrolysis, indicating that CGI-58 likely coactivates a DEUP- and E-600-sensitive TG lipase in CHO-K1 cells.

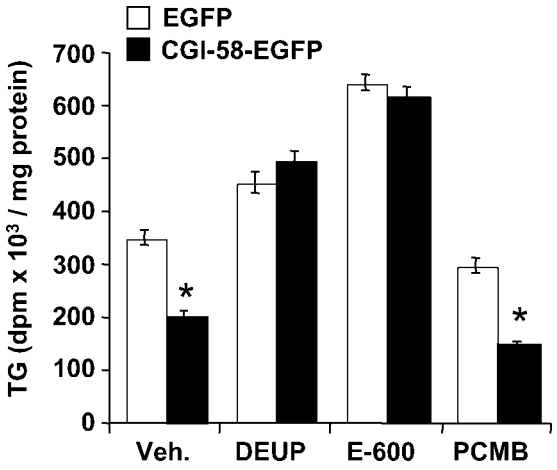

Fig. 4. CGI-58-driven TG hydrolysis is blocked by diethylumbelliferyl phosphate (DEUP) and diethyl-*p*-nitrophenyl phosphate (E-600) but not by *p*-chloro-mercuribenzoate (PCMB). CHO-K1 cell lines stably overexpressing either EGFP or CGI-58-EGFP were pretreated with either a vehicle (DMSO; Veh.) or 50 μg/ml DEUP, 500 μM E-600, or 25 μM PCMB for 1 h. Cells were then pulse-labeled with 5 μCi of [^{3}H]oleic acid in medium A for 4 h in the continued presence of inhibitors. Thereafter, the incorporation of [^{3}H]oleic acid into TG, CE, and PL was determined. Data represent means ± SEM (n = 4) from a representative experiment, which was repeated twice with similar results. * $P < 0.01$ (CGI-58-EGFP vs. EGFP cells).

CGI-58-driven TG hydrolysis is coupled to increased fatty acid oxidation

Because TG hydrolysis can potentially liberate free fatty acids for β-oxidation, we examined whether CGI-58-mediated hydrolysis was associated with increased fatty acid oxidation in several cell models. HepG2 cells transiently transfected (~50% efficiency) with CGI-58-EGFP exhibited a 2.6-fold increase in fatty acid oxidation (conversion of [^{14}C]oleic acid to [^{14}C]CO_2) compared with EGFP-transfected cells (**Fig. 5A**). In agreement, CHO-K1 cells stably expressing CGI-58-EGFP exhibited on average a 1.8-fold increase in fatty acid oxidation compared with EGFP cell lines (data not shown). Furthermore, siRNA-mediated knockdown of endogenous CGI-58 in McA-RH7777 cells resulted in a 32% reduction in fatty acid oxidation compared with cells treated with a nontargeting control siRNA (Fig. 5B). These data suggest that CGI-58-driven TG hydrolysis provides fatty acid substrate available for complete β-oxidation into CO_2.

CGI-58-driven hydrolysis of stored TG is coupled to increased lipoprotein TG secretion

The packaging of TG into nascent lipoprotein particles in hepatocytes relies on the lipolysis of cytoplasmic LD-stored TG and subsequent reesterification at the ER (3, 7, 8). To examine whether CGI-58 affected lipoprotein-associated TG secretion, CGI-58-EGFP fusion proteins were overexpressed in both McA-RH7777 and

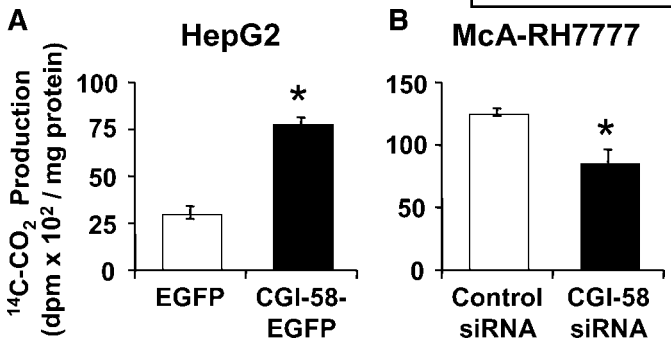

Fig. 5. CGI-58-driven TG hydrolysis is coupled to increased fatty acid oxidation. A: HepG2 cells were transiently transfected (~50% transfection efficiency) with plasmids encoding EGFP or CGI-58-EGFP fusion proteins. B: McA-RH7777 cells were transfected with either 100 nM of a nontargeting siRNA (Control siRNA) or a pool of siRNAs targeting the endogenous CGI-58 (CGI-58 siRNA). At 24 h after transfection, all cells were grown in serum-free medium for an additional 24 h. Thereafter, all cells were pulse-labeled with 0.5 μCi of [^{14}C]oleic acid in serum-free medium for 6 h in oxidation chambers, and the conversion of [^{14}C]oleic acid to [^{14}C]CO_2 was measured. Data represent means ± SEM (n = 4) from a representative experiment, which was repeated twice with similar results. * $P < 0.05$ (CGI-58-EGFP vs. EGFP cells or CGI-58 siRNA vs. Control siRNA).

HepG2 cells. As seen in **Fig. 6A**, modest transient overexpression (see supplementary Fig. II) of CGI-58-EGFP fusion proteins resulted in ~73% and ~10% increases in lipoprotein-associated (d < 1.225 g/ml media fraction) TG secretion in HepG2 and McA-RH7777 cells, respectively, compared with cells transfected with EGFP alone. To further study the role of CGI-58 in lipoprotein TG secretion, we used siRNA to reduce endogenous CGI-58 in McA-RH7777 cells (see supplementary Fig. II). As a result of siRNA-mediated silencing of endogenous CGI-58 (~60% decrease in mRNA and protein), TG secretion in VLDL-, IDL-, and LDL-sized particles (d < 1.063 g/ml) was reduced by 43% compared with control siRNA-treated cells (Fig. 6B). However, the secretion of TG into small dense lipoproteins (d > 1.063 g/ml) was not significantly altered by CGI-58 siRNA treatment (Fig. 6B).

To examine whether CGI-58 affects the packaging of stored TG (almost exclusively associated with cytoplasmic LDs) or TG being newly synthesized from an exogenous fatty acid source, siRNA-treated cells were pulse-labeled with [^{3}H]oleic acid for 24 h to label LD-associated stored TG pools and then chased with exogenous [^{14}C]oleic acid for an additional 4 h, and TG secretion was examined. Interestingly, siRNA-mediated knockdown of CGI-58 resulted in a 60% reduction in the packaging of stored (^{3}H-labeled) TG into nascent VLDL-, IDL-, and LDL-sized particles (d < 1.063 g/ml) compared with control siRNA-treated cells (Fig. 6C). In parallel, siRNA-mediated knockdown of CGI-58 resulted in a 59% reduction in the packaging of exogenous, newly synthesized TG into nascent VLDL-, IDL-, and LDL-sized particles (d < 1.063 g/ml). Collectively, these data demonstrate that CGI-58 plays a role in the lipolysis/

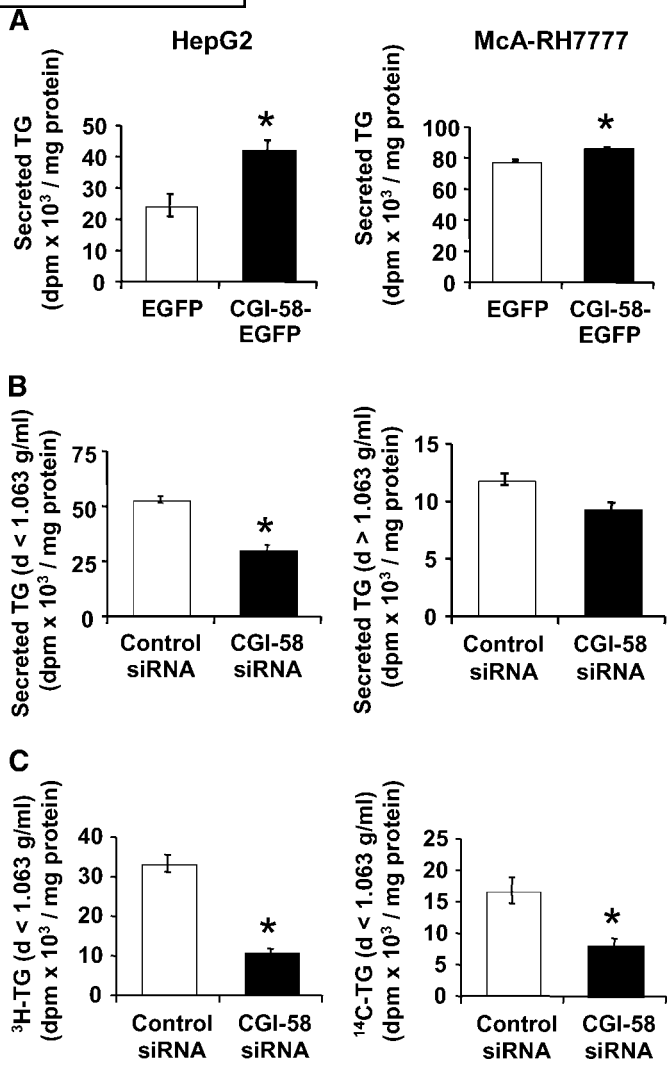

Fig. 6. CGI-58-driven hydrolysis of stored TG is coupled to increased secretion of TG-rich lipoproteins. A: McA-RH7777 and HepG2 hepatoma cells were transfected with plasmids encoding EGFP or CGI-58-EGFP fusion proteins. At 48 h after transfection, the cells were pulse-labeled with 5 μCi of [^{3}H]oleic acid for 4 h in medium B in the presence of 0.8 mM cold oleic acid. The incorporation of [^{3}H]oleic acid into lipoprotein-associated TG was determined. B: McA-RH7777 cells were transfected with either 100 nM of a nontargeting siRNA (Control siRNA) or a pool of siRNAs targeting the endogenous CGI-58 (CGI-58 siRNA). At 48 h after transfection, all cells were pulse-labeled with 5 μCi of [^{3}H]oleic acid for 4 h in medium B in the presence of 0.8 mM cold oleic acid. The incorporation of [^{3}H]oleic acid into lipoprotein-associated TG was determined as described in Materials and Methods. C: McA-RH7777 cells were transfected with either 100 nM nontargeting siRNA (Control siRNA) or a pool of siRNAs targeting the endogenous CGI-58 (CGI-58 siRNA). Twenty-four hours after transfection, all cells were pulse-labeled in medium B containing 5 μCi of [^{3}H]oleic acid for 24 h to label stored TG pools. Thereafter, all cells were chased in medium B containing 1 μCi of [^{14}C]oleic acid and 0.8 mM cold oleic acid to drive TG secretion. The incorporation of [^{3}H]oleic acid and [^{14}C]oleic acid into lipoprotein-associated TG pools was determined as described in Materials and Methods. Data represent means ± SEM (n = 3) from a representative experiment, which was repeated twice (A, C) or three times (B) with similar results. * $P < 0.05$ (CGI-58-EGFP vs. EGFP cells or CGI-58 siRNA vs. Control siRNA).

reesterification cycle in hepatoma cells that is known to be crucial for lipoprotein TG secretion.

DISCUSSION

This study provides, for the first time, evidence indicating that CGI-58 may drive the hydrolysis of stored TG for preferential shuttling into secreted TG-rich lipoprotein particles or oxidative pathways, thereby potentially limiting the extent of hepatic steatosis. The major findings in the model cell systems of this study are as follows: *1*) CGI-58 localizes to the ER, Golgi apparatus, and LD compartments in multiple cell models; and *2*) CGI-58 drives TG hydrolysis in multiple cell lines, which is dependent on DEUP- and E-600-sensitive TG lipase(s) and coupled to an increase in fatty acid oxidation and lipoprotein-TG secretion in hepatoma cells. These findings warrant further examination of CGI-58's role in lipoprotein TG secretion in whole animals.

The current study demonstrates that CGI-58-EGFP fusion proteins can localize to LDs, the ER, and the Golgi apparatus (Fig. 2), all of which are involved in the assembly of apoB-containing nascent lipoprotein particles and VLDL-TG secretion (7, 8). The fact that CGI-58-EGFP fusion proteins can concentrate to cytoplasmic LDs in response to oleate stimulation is important, because oleate supplementation promotes VLDL-TG secretion in most hepatoma cell lines (7, 8). In addition, CGI-58 is now a well-documented potent facilitator of hepatocyte TG hydrolysis (34, 35) (Fig. 3). Therefore, likely by coactivating a DEUP- and E-600-sensitive TG lipase (Fig. 4), CGI-58 facilitates the liberation of acylglycerol intermediates that are used for reesterification and packaging into secreted lipoprotein particles in hepatoma cells. All of these findings point to CGI-58 as a critical player in the second-step expansion of apoB-containing lipoproteins (9–12). However, additional work is needed to more clearly identify the intracellular itinerary of CGI-58 among LD, ER, and Golgi compartments and whether CGI-58 directly interacts with known components of apoB particle synthesis (i.e., MTP and apoB) (9–12).

In light of these findings regarding CGI-58's role in lipoprotein TG secretion, the abundant expression of CGI-58 in monkey small intestine (Fig. 1) makes it tempting to speculate that CGI-58 may play a similar role in chylomicron packaging in the intestinal enterocyte. Interestingly, thorough histological examination of the original patient presenting with CDS revealed marked lipid accumulation in the columnar absorptive cells in intestinal mucosa (15). The authors stated that this lipid accumulation resembled abetalipoproteinemia, a disease caused by mutations in MTP that presents as fat malabsorption and the virtual absence of apoB-containing lipoproteins in plasma (46). Hence, it would be of interest to examine patients with CDS for fat and vitamin malabsorption and its relationship to clinical manifestations.

Although CGI-58 may play a critical role in the packaging of apoB-containing lipoproteins in hepatocytes and enterocytes, it most assuredly does not have this same role in the many other tissues in which it is expressed (Fig. 1). One consistent finding is that CGI-58 facilitates TG hydrolysis in almost all cell types examined (34, 35) (Fig. 3). Hence, CGI-58's primary role seems to be as a coactivator for ATGL and other as yet unidentified lipases, because CGI-58 itself lacks a critical serine in its catalytic domain, which renders it incapable of intrinsic TG hydrolytic activity (34, 35).

Indeed, facilitating TG hydrolysis is likely to be CGI-58's primary role, yet the acylglycerol intermediates and fatty acids liberated may be handled in a cell type-specific manner. For example, in most cell types, including fibroblasts, hydrolysis of TG typically generates acylglycerol intermediates that can be preferentially used for PL synthesis (5, 6). Therefore, the elegant work done by Igal and Coleman (25, 26), demonstrating that fibroblasts from CDS patients had defective recycling of TG-derived acylglycerols to PLs, reflects the importance of CGI-58 in this process in fibroblasts. In contrast, acylglycerols and fatty acids liberated from TG hydrolysis in hepatocytes are used for *1*) VLDL packaging through reesterification at the ER, *2*) β-oxidation of fatty acids for local energy needs, or *3*) ketone body generation to supply alternative energy for other tissues during the starved state (3, 7, 8). Hence, our finding that both fatty acid oxidation (Fig. 5) and packaging of TG into secreted lipoproteins (Fig. 6) was facilitated by CGI-58 in hepatoma cells is consistent with the typical pattern of substrate utilization in these cells. Collectively, we believe that acylglycerols and fatty acids liberated by CGI-58-driven TG hydrolysis may be preferentially sent toward the secretory pathway in cells expressing apoB and MTP or may be sent toward either oxidative or PL recycling pathways in other cells types. More work is required to address these possibilities.

Another important question raised by our work is which TG hydrolase is responsible for CGI-58-mediated lipolysis in hepatocytes, because ATGL and hormone-sensitive lipase are likely not expressed well in the liver (34, 47, 48). It has been demonstrated previously that two known TG hydrolases can function to couple TG hydrolysis to VLDL packaging. The first enzyme described with this distinction was a hepatic microsomal lipase named triacylglycerol hydrolase, which promotes VLDL-TG secretion in transfected McA-RH7777 cells (49, 50). Another candidate lipase is arylacetamide deacetylase, which is highly homologous to hormone-sensitive lipase and also has been shown to augment TG secretion in transfected HepG2 cells (3, 51). Even with these obvious candidates, one cannot rule out ATGL as a potential TG hydrolase in hepatocytes, because ATGL-deficient mice display a 2.3-fold increase in hepatic TG content (52). In further support of this concept, ATGL has several other names, including transport secretion protein, desnutrin, and, more importantly, calcium-independent phospholipase A2ζ (iPLA2ζ), which is a member of the iPLA2/lipase subfamily (53). Intriguingly, inhibition of iPLA2 function in McA-RH7777 cells resulted in reductions in VLDL-TG secretion (54), strikingly similar to what was seen in our siRNA-mediated knockdown of CGI-58 (Fig. 6).

These data indicate that additional studies are warranted to define whether CGI-58 coactivates ATGL or other lipases in the liver and how this interaction occurs spatially.

In conclusion, our studies demonstrate for the first time that CGI-58 functions to promote TG hydrolysis in multiple cell models, likely by coactivating DEUP- and E-600-sensitive TG lipases. Importantly, in hepatoma cells, CGI-58-driven TG hydrolysis is coupled to both increased fatty acid oxidation and packaging of TG into lipoproteins. These findings demonstrate an important role of CGI-58 in regulating lipoprotein TG secretion in hepatocytes, yet they raise many new questions about the molecular details of CGI-58-driven lipolysis. For example, would mice lacking CGI-58 be obese or would they present more like humans with CDS (i.e., ichthyosis, hepatic steatosis, cardiomyopathy, etc.)? Conversely, would mice overexpressing this protein in adipose or liver be lean or be protected against hepatic steatosis, respectively? Is ATGL the only lipase that CGI-58 coactivates, or are other lipases involved in a tissue-specific manner? Does CGI-58-mediated TG hydrolysis generate signaling-competent lipid intermediates (diacylglycerols, phosphatidic acid, lysophosphatidic acid, etc.) that could mediate lipid-induced insulin resistance? Studies are currently under way to address these questions, and they should provide a framework for a more complete understanding of TG hydrolysis and its role in normal lipid homeostasis as well as pathophysiologic states such as the metabolic syndrome.

The authors are grateful to Dr. Dawn Brasaemle (Rutgers University) for insightful discussion and provision of antisera raised against mouse CGI-58. The authors thank Dr. Takashi Osumi (University of Hyogo) for providing antisera raised against rat CGI-58. The authors also thank Dr. Michael McIntosh (University of North Carolina at Greensboro) for generously providing primary human adipocyte RNA for cloning purposes. This work was supported by grants from the American Heart Association (Postdoctoral Fellowship 0625400U to J.M.B. and a Scientist Development Grant 0635261N to L.Y.) and the National Institutes of Health (Grant P01 HL-49373 to L.L.R. and G.S.).

REFERENCES

1. Liu, P., Y. Ying, Y. Zhao, D. I. Mundy, M. Zhu, and R. G. Anderson. 2004. Chinese hamster ovary K2 cell lipid droplets appear to be metabolic organelles involved in membrane traffic. *J. Biol. Chem.* **279:** 3787–3792.
2. Murphy, D. J., and J. Vance. 1999. Mechanisms of lipid-body formation. *Trends Biochem. Sci.* **24:** 109–115.
3. Gibbons, G. F., K. Islam, and R. J. Pease. 2000. Mobilisation of triacylglycerol stores. *Biochim. Biophys. Acta.* **1483:** 37–57.
4. Murphy, D. J. 2001. The biogenesis and functions of lipid bodies in animals, plants and microorganisms. *Prog. Lipid Res.* **40:** 325–438.
5. Cook, H. W., and M. W. Spence. 1985. Triacylglycerol as a precursor in phospholipid biosynthesis in cultured neuroblastoma cells: studies with labeled glucose, fatty acid, and triacylglycerol. *Can. J. Biochem. Cell Biol.* **63:** 919–926.
6. Igal, R. A., P. Wang, and R. A. Coleman. 1997. Triacsin C blocks de novo synthesis of glycerolipids and cholesterol esters but not recycling of fatty acid into phospholipid: evidence for functionally separate pools of acyl-CoA. *Biochem. J.* **324:** 529–534.
7. Shelness, G. S., and A. S. Ledford. 2005. Evolution and mechanism of apolipoprotein B-containing lipoprotein assembly. *Curr. Opin. Lipidol.* **16:** 325–332.
8. Gibbons, G. F., D. Wiggins, A. M. Brown, and A. M. Hebbachi. 2004. Synthesis and function of hepatic very-low-density lipoprotein. *Biochem. Soc. Trans.* **32:** 59–64.
9. Bar-On, H., P. S. Roheim, O. Stein, and Y. Stein. 1971. Contribution of floating fat triglyceride and of lecithin towards formation of secretory triglyceride in perfused rat liver. *Biochim. Biophys. Acta.* **248:** 1–11.
10. Alexander, C. A., R. L. Hamilton, and R. J. Havel. 1976. Subcellular localization of B apoprotein of plasma lipoproteins in rat liver. *J. Cell Biol.* **69:** 241–263.
11. Mooney, R. A., and M. D. Lane. 1981. Formation and turnover of triglyceride-rich vesicles in the chick liver cell. Effects of cAMP and carnitine on triglyceride mobilization and conversion to ketones. *J. Biol. Chem.* **256:** 11724–11733.
12. Francone, O. L., A. D. Kalopissis, and G. Griffaton. 1989. Contribution of cytoplasmic storage triacylglycerol to VLDL-triacylglycerol in isolated rat hepatocytes. *Biochim. Biophys. Acta.* **1002:** 28–36.
13. Chanarin, I., A. Patel, G. Slavin, E. J. Wills, T. M. Andrews, and G. Stewart. 1975. Neutral-lipid storage disease: a new disorder of lipid metabolism. *BMJ.* **1:** 553–555.
14. Dorfman, M. L., C. Hershko, S. Eisenberg, and F. Sagher. 1974. Ichthyosiform dermatosis with systemic lipidosis. *Arch. Dermatol.* **110:** 261–266.
15. Slavin, G., E. J. Wills, J. E. Richmond, I. Chanarin, T. Andrews, and G. Stewart. 1975. Morphological features in a neutral lipid storage disease. *J. Clin. Pathol.* **28:** 701–710.
16. Mela, D., A. Artom, R. Goretti, G. Varagona, M. Riolfo, S. Ardoino, G. Sanguineti, A. Vitali, and S. Ricciardi. 1996. Dorfman-Chanarin syndrome: a case with prevalent hepatic involvement. *J. Hepatol.* **25:** 769–771.
17. Igal, R. A., J. M. Rhoads, and R. A. Coleman. 1997. Neutral lipid storage disease with fatty liver and cholestasis. *J. Pediatr. Gastroenterol. Nutr.* **25:** 541–547.
18. Srebrnik, A., S. Brenner, B. Ilie, and G. Messer. 1998. Dorfman-Chanarin syndrome: morphologic studies and presentation of new cases. *Am. J. Dermatopathol.* **20:** 79–85.
19. Radom, J., R. Salvayre, A. Negre, and L. Douste-Blazy. 1989. Metabolism of pyrenedecanoic acid in Epstein-Barr virus-transformed lymphoid cell lines from normal subjects and from a patient with multisystemic lipid storage myopathy. *Biochim. Biophys. Acta.* **1005:** 130–136.
20. Williams, M. L., D. J. Monger, S. L. Rutherford, M. Hincenbergs, S. J. Rehfeld, and C. Grunfeld. 1988. Neutral lipid storage disease with ichthyosis: lipid content and metabolism of fibroblasts. *J. Inherit. Metab. Dis.* **11:** 131–143.
21. Salvayre, R., A. Negre, J. Radom, and L. Douste-Blazy. 1989. Independence of triacylglycerol-containing compartments in cultured fibroblasts from Wolman disease and multisystemic lipid storage myopathy. *FEBS Lett.* **250:** 35–39.
22. Williams, M. L., R. A. Coleman, D. Placezk, and C. Grunfeld. 1991. Neutral lipid storage disease: a possible functional defect in phospholipid-linked triacylglycerol metabolism. *Biochim. Biophys. Acta.* **1096:** 162–169.
23. Hilaire, N., A. Negre-Salvayre, and R. Salvayre. 1994. Cellular uptake and catabolism of high-density-lipoprotein triacylglycerols in human cultured fibroblasts: degradation block in neutral lipid storage disease. *Biochem. J.* **297:** 467–473.
24. Hilaire, N., R. Salvayre, J. C. Thiers, M. J. Bonnafe, and A. Negre-Salvayre. 1995. The turnover of cytoplasmic triacylglycerols in human fibroblasts involves two separate acyl chain length-dependent degradation pathways. *J. Biol. Chem.* **270:** 27027–27034.
25. Igal, R. A., and R. A. Coleman. 1996. Acylglycerol recycling from triacylglycerol to phospholipid, not lipase activity, is defective in neutral lipid storage disease fibroblasts. *J. Biol. Chem.* **271:** 16644–16651.
26. Igal, R. A., and R. A. Coleman. 1998. Neutral lipid storage disease: a genetic disorder with abnormalities in the regulation of phospholipid metabolism. *J. Lipid Res.* **39:** 31–43.
27. Lefevre, C., F. Jobard, F. Caux, B. Bouadjar, A. Karaduman, R. Heilig, H. Lakhdar, A. Wollenberg, J. L. Verret, J. Weissenbach, et al. 2001. Mutations in CGI-58, the gene encoding a new protein of the esterase/lipase/thioesterase subfamily, in Chanarin-Dorfman syndrome. *Am. J. Hum. Genet.* **69:** 1002–1012.
28. Akiyama, M., D. Sawamura, Y. Nomura, M. Sugawara, and H. Shimizu. 2003. Truncation of CGI-58 protein causes malformation

of lamellar granules resulting in ichthyosis in Dorfman-Chanarin syndrome. *J. Invest. Dermatol.* **121:** 1029–1034.
29. Caux, F., Z. B. Selma, L. Laroche, J. F. Prud'homme, and J. Fischer. 2004. CGI-58/ABHD5 gene is mutated in Dorfman-Chanarin syndrome. *Am. J. Med. Genet. A.* **129:** 214.
30. Srinivasan, R., N. Hadzic, J. Fischer, and A. S. Knisely. 2004. Steatohepatitis and unsuspected micronodular cirrhosis in Dorfman-Chanarin syndrome with documented ABHD5 mutation. *J. Pediatr.* **144:** 662–665.
31. Selma, Z. B., S. Yilmaz, P. O. Schischmanoff, A. Blom, C. Ozogul, L. Laroche, and F. Caux. 2007. A novel S115G mutation of CGI-58 in a Turkish patient with Dorfman-Chanarin syndrome. *J. Invest. Dermatol.* In press.
32. Yamaguchi, T., N. Omatsu, S. Matsushita, and T. Osumi. 2004. CGI-58 interacts with perilipin and is localized to lipid droplets. Possible involvement of CGI-58 mislocalization in Chanarin-Dorfman syndrome. *J. Biol. Chem.* **279:** 30490–30497.
33. Subramanian, V., A. Rothenberg, C. Gomez, A. W. Cohen, A. Garcia, S. Bhattacharyya, L. Shapiro, G. Dolios, R. Wang, M. P. Lisanti, et al. 2004. Perilipin A mediates the reversible binding of CGI-58 to lipid droplets in 3T3-L1 adipocytes. *J. Biol. Chem.* **279:** 42062–42071.
34. Lass, A., R. Zimmermann, G. Haemmerle, M. Riederer, G. Schoiswohl, M. Schweiger, P. Kienesberger, J. G. Strauss, G. Gorkiewicz, and R. Zechner. 2006. Adipose triglyceride lipase-mediated lipolysis of cellular fat stores is activated by CGI-58 and defective in Chanarin-Dorfman syndrome. *Cell Metab.* **3:** 309–319.
35. Yamaguchi, T., N. Omatsu, E. Morimoto, H. Nakashima, K. Ueno, T. Tanaka, K. Satouchi, F. Hirose, and T. Osumi. 2007. CGI-58 facilitates lipolysis on lipid droplets but is not involved in the vesiculation of lipid droplets caused by hormonal stimulation. *J. Lipid Res.* **48:** 1078–1089.
36. Bligh, E. G., and W. J. Dyer. 1959. A rapid method of total lipid extraction and purification. *Can. J. Biochem. Physiol.* **37:** 911–917.
37. Yu, L., S. Bharadwaj, J. M. Brown, Y. Ma, W. Du, M. A. Davis, P. Michaely, P. Liu, M. C. Willingham, and L. L. Rudel. 2006. Cholesterol-regulated translocation of NPC1L1 to the cell surface facilitates free cholesterol uptake. *J. Biol. Chem.* **281:** 6616–6624.
38. Moreau, H., A. Moulin, Y. Gargouri, J. P. Noel, and R. Verger. 1991. Inactivation of gastric and pancreatic lipases by diethyl p-nitrophenyl phosphate. *Biochemistry.* **30:** 1037–1041.
39. Harrison, E. H., D. W. Bernard, P. Scholm, D. M. Quinn, G. H. Rothblat, and J. M. Glick. 1990. Inhibitors of neutral cholesteryl ester hydrolase. *J. Lipid Res.* **31:** 2187–2193.
40. Delamatre, J. G., R. M. Carter, and C. A. Hornick. 1993. Evidence that a neutral cholesteryl ester hydrolase is responsible for the extralysosomal hydrolysis of high-density lipoprotein cholesteryl ester in rat hepatoma cells (Fu5AH). *J. Cell. Physiol.* **157:** 164–168.
41. Brown, J. M., M. S. Boysen, S. S. Jensen, R. F. Morrison, J. Storkson, R. Lea-Currie, M. Pariza, S. Mandrup, and M. K. McIntosh. 2003. Isomer-specific regulation of metabolism and PPARgamma signaling by CLA in human preadipocytes. *J. Lipid Res.* **44:** 1287–1300.
42. Brown, J. M., M. S. Boysen, S. Chung, O. Fabiyi, R. F. Morrison, S. Mandrup, and M. K. McIntosh. 2004. Conjugated linoleic acid induces human adipocyte delipidation: autocrine/paracrine regulation of MEK/ERK signaling by adipocytokines. *J. Biol. Chem.* **279:** 26735–26747.
43. Yu, L., J. Li-Hawkins, R. E. Hammer, K. E. Berge, J. D. Horton, J. C. Cohen, and H. H. Hobbs. 2002. Overexpression of ABCG5 and ABCG8 promotes biliary cholesterol secretion and reduces fractional absorption of dietary cholesterol. *J. Clin. Invest.* **110:** 671–680.
44. Temel, R. E., R. G. Lee, K. L. Kelley, M. A. Davis, R. Shah, J. K. Sawyer, M. D. Wilson, and L. L. Rudel. 2005. Intestinal cholesterol absorption is substantially reduced in mice deficient in both ATP-binding cassette transporter A1 (ABCA1) and acyl-CoA:cholesterol O-acyltransferase 2 (ACAT2). *J. Lipid Res.* **46:** 2423–2431.
45. Xu, G., C. Sztalryd, X. Lu, J. T. Tansey, J. Gan, H. Dorward, A. R. Kimmel, and C. Londos. 2005. Post-translational regulation of adipose differentiation-related protein by the ubiquitin/proteasome pathway. *J. Biol. Chem.* **280:** 42841–42847.
46. Hooper, A. J., F. M. van Bockxmeer, and J. R. Burnett. 2005. Monogenic hypocholesterolaemic lipid disorders and apolipoprotein B metabolism. *Crit. Rev. Clin. Lab. Sci.* **42:** 515–545.
47. Zimmermann, R., J. G. Strauss, G. Haemmerle, G. Schoiswohl, R. Birner-Gruenberger, M. Riederer, A. Lass, G. Neuberger, F. Eisenhaber, A. Hermetter, et al. 2004. Fat mobilization in adipose tissue is promoted by adipose triglyceride lipase. *Science.* **306:** 1383–1386.
48. Holm, C., P. Belfrage, and G. Fredrikson. 1987. Immunological evidence for the presence of hormone-sensitive lipase in rat tissues other than adipose tissue. *Biochem. Biophys. Res. Commun.* **148:** 99–105.
49. Lehner, R., and D. E. Vance. 1999. Cloning and expression of a cDNA encoding a hepatic microsomal lipase that mobilizes stored triacylglycerol. *Biochem. J.* **343:** 1–10.
50. Lehner, R., Z. Cui, and D. E. Vance. 1999. Subcellullar localization, developmental expression and characterization of a liver triacylglycerol hydrolase. *Biochem. J.* **338:** 761–768.
51. Trickett, J. I., D. D. Patel, B. L. Knight, E. D. Saggerson, G. F. Gibbons, and R. J. Pease. 2001. Characterization of the rodent genes for arylacetamide deacetylase, a putative microsomal lipase, and evidence for transcriptional regulation. *J. Biol. Chem.* **276:** 39522–39532.
52. Haemmerle, G., A. Lass, R. Zimmermann, G. Gorkiewicz, C. Meyer, J. Rozman, G. Heldmaier, R. Maier, C. Theussl, S. Eder, et al. 2006. Defective lipolysis and altered energy metabolism in mice lacking adipose triglyceride lipase. *Science.* **312:** 734–737.
53. Jenkins, C. M., D. J. Mancuso, W. Yan, H. F. Sims, B. Gibson, and R. W. Gross. 2004. Identification, cloning, expression, and purification of three novel human calcium-independent phospholipase A2 family members possessing triacylglycerol lipase and acylglycerol transacylase activities. *J. Biol. Chem.* **279:** 48968–48975.
54. Tran, K., Y. Wang, C. J. DeLong, Z. Cui, and Z. Yao. 2000. The assembly of very low density lipoproteins in rat hepatoma McA-RH7777 cells is inhibited by phospholipase A2 antagonists. *J. Biol. Chem.* **275:** 25023–25030.